Charge transport in lithium phthalocyanine

Michael Dumm, Peter Lunkenheimer, Alois Loidl, B. Assmann, H. Homborg, P. Fulde

Angaben zur Veröffentlichung / Publication details:

Dumm, Michael, Peter Lunkenheimer, Alois Loidl, B. Assmann, H. Homborg, and P. Fulde. 1996. "Charge transport in lithium phthalocyanine." The Journal of Chemical Physics 104 (13): 5048–53. https://doi.org/10.1063/1.471134.

The Journal of Chemical Physics

RESEARCH ARTICLE | APRIL 01 1996

Charge transport in lithium phthalocyanine

M. Dumm; P. Lunkenheimer; A. Loidl; B. Assmann; H. Homborg; P. Fulde

J. Chem. Phys. 104, 5048–5053 (1996)
https://doi.org/10.1063/1.471134

AIP Publishing

Charge transport in lithium phthalocyanine

M. Dumm, P. Lunkenheimer, and A. Loidl
Institut für Festkörperphysik, Technische Hochschule Darmstadt, D-64289 Darmstadt, Germany

B. Assmann and H. Homborg
Institut für anorganische Chemie, Christian-Albrechts-Universität, D-24098 Kiel, Germany

P. Fulde
Max-Planck-Institut für Physik komplexer Systeme, D-01187 Dresden, Germany

(Received 16 November 1995; accepted 22 December 1995)

The ac electrical properties of monoclinic lithium phthalocyanine (LiPc) and of the iodinated compound LiPcI have been investigated in the frequency and temperature regimes 20 Hz$\leqslant\nu\leqslant$1 GHz and 1.5 K$\leqslant T\leqslant$300 K, respectively. Both compounds are semiconductors with dielectric constants $\epsilon_\infty\approx$6 (LiPc) and 20 (LiPcI). Up to room temperature tunneling of charge carriers is the dominant conduction process in both compounds, yielding intrinsic dc conductivities $\sigma_{dc}\approx 5.3\times10^{-4}\ \Omega^{-1}\,cm^{-1}$ (LiPc) and 0.2 $\Omega^{-1}\,cm^{-1}$ (LiPcI). The frequency and temperature dependence of the complex ac conductivity suggests polarons as the dominant species of charge carriers. The higher conductivity of the iodinated compound can be attributed to an enhanced mobility of the polaronic charge carriers which is most probably due to a better overlap of the π orbitals along the stacking direction of the molecules. © *1996 American Institute of Physics.* [S0021-9606(96)51612-4]

I. INTRODUCTION

For many years the strong interest in metallophthalocyanines originated mainly from their application as coloring pigments. However, in recent years these substances found renewed attention because they are promising materials for a variety of technical applications as, e.g., constituents of molecular electronics, electrochromic devices, gas sensors, and magnetic materials (see e.g. Ref. 1). Depending on composition and doping level, the electrical properties of the metallophthalocyanines vary markedly exhibiting insulating (e.g., H_2Pc, CuPc, NiPc), semiconducting (e.g., $LuPc_2$, LiPc), or, when doped with an oxidizing material, even metallic behavior (e.g., H_2PcI, NiPcI, CuPcI). LiPc and $LuPc_2$ which both have unpaired electrons are the only nonoxidized phthalocyanines with a relatively high conductivity in the semiconducting range.[2] Band structure calculations of LiPc predicted a half-filled conduction band.[3] An explanation of the semiconducting properties of this material is the formation of a Mott–Hubbard gap due to Coulomb repulsion of the unpaired electrons.[4]

Phthalocyanines consist of macrocyclic molecules containing four pyrrole units which are connected by $-N=$ bridges and linked to one benzole unit each. In the inner macrocycle there are two NH groups, the H atoms of which can be substituted by a metal atom. In LiPc the lithium ion is located at the centre of the inner cycle with both H atoms removed which leaves an unpaired electron. This electron has been found to be delocalized on the inner ring of the macrocycle.[5] In the metallophthalocyanines the molecules form stacks along the *c* axis. LiPc is known to form a monoclinic or tetragonal crystal structure.[6,7] If it is doped by halogens only the tetragonal modification is stable.[6] LiPc, as all the other metallophthalocyanines, is effectively a one-dimensional conductor with the conduction path along the stacking direction of the molecules which is due to a considerable overlap of the π orbitals in this direction.[8]

Doping of metallophthalocyanines with halogens (usually iodine) induces an enhancement of the electrical conductivity over several orders of magnitude and in some cases can even cause a transition into a metallic state.[9–11] Various possible explanations for this finding have been proposed: (i) The phthalocyanine molecule is partially oxidized leading to holes in the lower Hubbard band.[12] (ii) The doping leads to a change of structure, e.g., from monoclinic to tetragonal as observed in NiPcI films,[11] which causes an enhanced overlap of the π orbitals.[8,11] (iii) The doping suppresses a Peierls metal–nonmetal transition and therefore the material remains metallic down to low temperatures.[6,10]

Measurements of the electrical properties of tetragonal LiPc have been performed previously by Turek *et al.*[2,13] The dc conductivity has been investigated between 140 K and room temperature and was found to behave thermally activated with an energy barrier of 0.16 eV and a room temperature conductivity of $\sigma_{dc}=2\times10^{-3}\ \Omega^{-1}\,cm^{-1}$.[2] In addition, the conductivity at 10 GHz has been reported[13] which is approximately one decade higher than the dc conductivity. For monoclinic LiPc and for LiPcI to our knowledge up to now only the dc conductivity at room temperature has been reported.[6]

We performed measurements of the complex conductivity and dielectric constant of monoclinic LiPc and of tetragonal LiPcI in a broad frequency range of 20 Hz$\leqslant\nu\leqslant$1 GHz and at temperatures 1.5 K$\leqslant T\leqslant$300 K. The aim of this investigation is to clarify the mechanism of charge transport and the nature of the charge carriers in these materials. In addition, by comparing the results for the two compounds, information on the mechanism of the conductivity enhancement in the iodine doped compound should be obtained.

 0021-9606/96/104(13)/5048/6/$10.00

II. EXPERIMENTAL DETAILS

For the synthesis of LiPc, 12.0 g of double distilled 1,2-dicyanobenzene (PDN) and 150 mg Li were heated to 150 °C. The exothermic reaction was finished within some minutes. After extraction of the reaction product with toluene, then acetone black needles of LiPc remained in the residue. For the synthesis of LiPcI, 10.0 g of double distilled PDN and 1.0 g LiI were heated to 145 °C for 15 h. After extraction of the reaction product with dichloromethane and ether lustrous needles of LiPcI remained. Both products gave satisfactory elemental analysis. The LiPc and LiPcI powders were pressed into pellets with a diameter of 6 mm. Sputtered gold contacts were applied on opposite sides of the pellets.

In the frequency range 20 Hz$\leqslant\nu\leqslant$1 MHz the measurements of the real part σ' and the imaginary part σ'' of the complex conductivity were carried out by using a fully automated autobalance bridge (HP 4284A). For frequency dependent measurements above 1 MHz the sample has been placed at the end of a coaxial line, connecting the inner and outer conductors. The complex reflection coefficient Γ of this assembly was measured by employing an HP 4191A impedance analyzer.[14] The complex conductivity can be determined from the complex reflection coefficient after the influence of the sample holder and the coaxial line has been eliminated by calibrating with three reference impedance terminations. All measurements reported in this work were done in two point technique.

The experiments were performed in a ^{4}He bath cryostat. The physical properties of the metallophthalocyanines are reported to be highly sensitive to absorbed oxygen which, however, is easily removed in vacuum.[13,15–17] Therefore, before the measurement was started, we applied for some hours a vacuum to the inner tube of the cryostat containing the sample in order to remove the absorbed oxygen.

III. RESULTS AND DISCUSSION

Figure 1 shows the temperature dependence of the dielectric constant ϵ' (a) and the conductivity σ' (b) for undoped LiPc as measured for various frequencies (double-logarithmic plot). ϵ' has been calculated from the measured σ'' by the relation $\epsilon'=\sigma''/(\omega\epsilon_0)$ where ϵ_0 is the dielectric constant of the vacuum and $\omega=2\pi\nu$. With increasing temperature both, $\epsilon'(T)$ and $\sigma'(T)$, increase by several orders of magnitude. For high temperatures all $\sigma'(T)$ curves approach the one obtained for 20 Hz which represents the dc limit. At lower temperatures $\sigma'(T)$ follows approximately a power law behavior, T^n with $n\approx3.8$. With decreasing temperature and for large frequencies the $\epsilon'(T)$ curves approach a saturation value of $\epsilon_\infty\approx6(\pm0.5)$ (see the results for $\nu\geqslant1$ MHz). The low frequency measurements ($\nu<1$ MHz) lead to a somewhat higher value (≈8) which is due to the stray capacitance of the cables. For temperatures $T>40$ K, $\epsilon'(T)$ exhibits a steplike increase over more than two decades which shifts to successively higher temperatures when the frequency is increased.

Figure 2 shows the same plot for LiPcI. The conductivity $\sigma'(T)$ exhibits a qualitatively similar behavior compared to

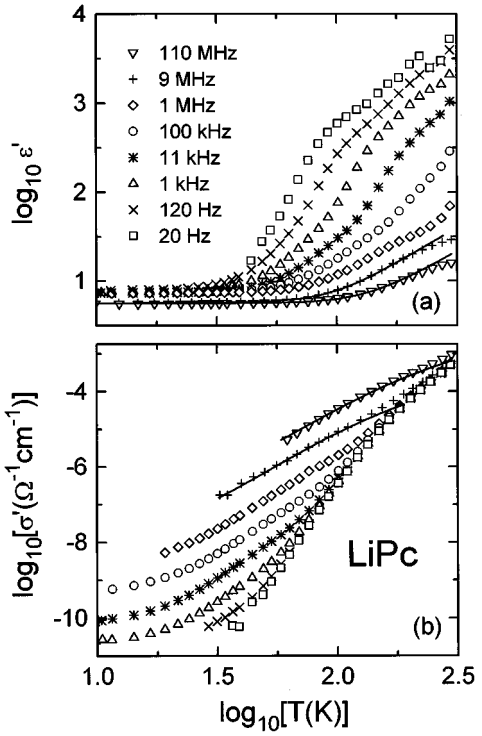

FIG. 1. Temperature dependence of the real parts of the dielectric constant (a) and the conductivity (b) of LiPc for various frequencies (double-logarithmic plots). The solid lines are the results of fits using the OLPT model predictions, Eqs. (2) and (3).

that obtained in LiPc, however with a clearly enhanced absolute value and a smaller temperature exponent, i.e., here $n\approx2$. The function $\epsilon'(T)$ approaches a saturation value for low temperatures of $\epsilon_\infty\approx20(\pm2)$, which is significantly higher than that for LiPc. For higher temperatures, $\epsilon'(T)$ increases by more than four decades in two successive steps which both shift to higher temperatures as the measuring frequency is increased.

In order to obtain better insight into this seemingly complicated behavior, we have plotted in Figs. 3 and 4 the frequency dependences of real and imaginary part of the conductivity for both materials in a double-logarithmic representation. The curves in Figs. 3 and 4 are composed of two sets of data each (for $\nu\leqslant1$ MHz and $\nu\geqslant1$ MHz) which in the case of LiPcI have been obtained on two different samples. Although in both cases the two data sets have not been shifted with respect to each other they match remarkedly well. Again a qualitatively similar behavior of doped and undoped LiPc is observed: $\sigma'(T)$ approaches a saturation value for low frequencies but increases at higher frequencies according to a power law. A power law behavior is often found in disordered conductors such as amorphous or doped semiconductors or ionic conductors and is usually ascribed to charge transport by hopping processes[18–20] between localized states. The frequency dependent conductivity can be parametrized according to $\sigma'=\sigma_{dc}+\sigma_0(\omega/\omega_0)^s$ for which the expression "universal dielectric response" (UDR) has been applied.[20] Here σ_{dc} denotes the dc conductivity and ω_0

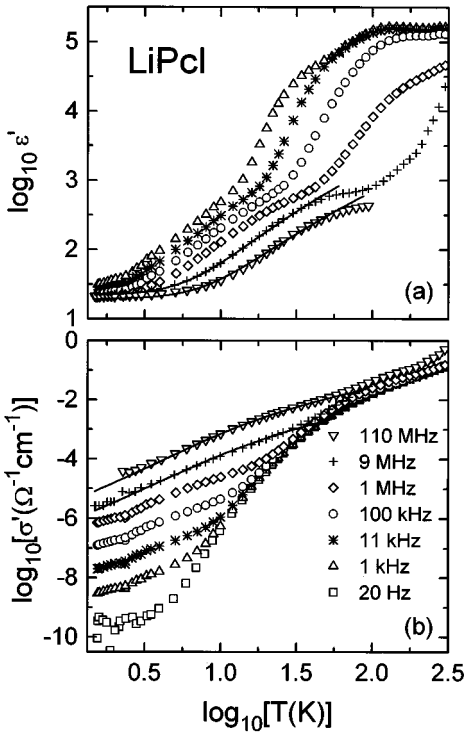

FIG. 2. Temperature dependence of the real parts of the dielectric constant (a) and the conductivity (b) of LiPcI for various frequencies (double-logarithmic plots). The solid lines are the results of fits using the OLPT model predictions, Eqs. (2) and (3).

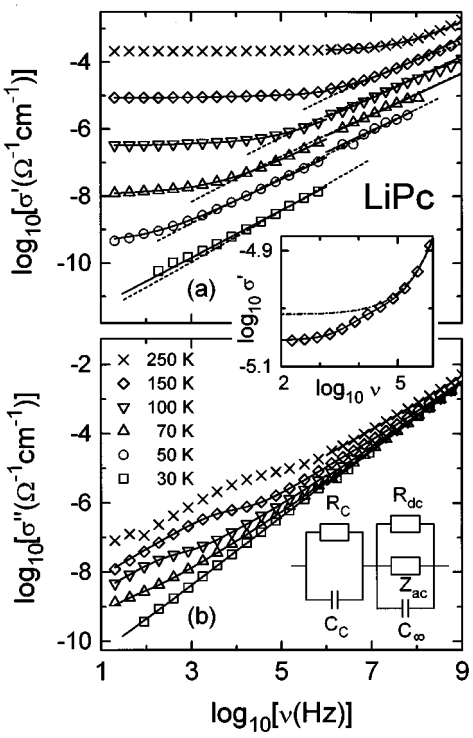

FIG. 3. Frequency dependence of real (a) and imaginary (b) part of the conductivity of LiPc for various temperatures. The solid lines are the results of fits using the UDR or the equivalent circuit indicated in the figure. Here C_c and R_c describe the contact contributions, R_{dc} and Z_{ac} the UDR behavior of the sample and C_∞ takes into account its high-frequency dielectric constant. The dashed lines in (a) have been calculated according to the OLPT model predictions [Eqs. (1) and (2)] with the parameters obtained from the OLPT fits of the temperature dependent data (Figs. 1 and 2). The inset shows an enlarged view of the behavior at low frequencies at 150 K. The dash–dotted line shows the intrinsic behavior without contacts.

is a reference frequency. Using the Kramers–Kronig relation and taking into account the high-frequency limit of the dielectric constant, ϵ_∞, the frequency dependence of the imaginary part can be written as: $\sigma''=\tan(s\pi/2)\sigma_0(\omega/\omega_0)^s+\epsilon_0\epsilon_\infty\omega$. Indeed, at high frequencies $\sigma''(\nu)$ shows a linear frequency behavior with slope 1 in the double-logarithmic representation of Figs. 3(b) and 4(b) which can be attributed to ϵ_∞. At lower frequencies the slope of $\sigma''(\nu)$ changes to a smaller value as is seen in Fig. 4(b) for 10 K. A detailed discussion of the exponent $s<1$ and its temperature dependence is given below. However, at temperatures $T\geqslant 100$ K for LiPc and $T\geqslant 20$ K for LiPcI a peak seems to be superimposed on the data which shifts to higher frequencies with increasing temperature. This feature is accompanied by a small steplike increase in $\sigma'(\nu)$ (see insets in Figs. 3 and 4) and can be ascribed to contributions of the contacts. Metal-semiconductor contacts usually exhibit high ohmic resistances accompanied by a high capacitance and often can be modeled by a circuit consisting of a resistance connected in parallel to a capacitance. We have performed least square fits of $\sigma'(\nu)$ and (simultaneously) $\sigma''(\nu)$ by assuming "pure" UDR behavior (including ϵ_∞) or the equivalent circuit shown in Fig. 3. It consists of an RC-circuit representing the contacts which is connected in series to the intrinsic sample impedance (UDR plus ϵ_∞). This circuit has been applied for data sets where the contacts contribute significantly to the results of the measurement (i.e., at high temperatures and low frequencies). The high and low frequency results have been fitted independently as the slight offsets between both data sets would influence the fit results. In addition, fits have only been performed for data sets at temperatures where the frequency response is not totally dominated by the contact contributions. The results of the fitting procedures are shown as solid lines in Figs. 3 and 4. Fits and data agree reasonably well which confirms the correctness of the assumed equivalent circuit. The deviations at high frequencies ($\nu>100$ MHz) and low temperatures are due to systematic errors occurring in the measurement of conductivities $\sigma'<10^{-5}$ Ω^{-1} cm^{-1} at these frequencies. In the insets of Figs. 3 and 4 the influence of the contacts is clearly demonstrated by comparing the fits with and without contacts: At low frequencies the contacts contribute significantly to the measured conductivity but with increasing frequency they become successively shorted by the contact-capacitance which leads to a steplike increase of $\sigma'(\nu)$. For LiPc the contact resistance R_c varies between 80 Ω at room temperature and 1 MΩ at 70 K and the contact capacitance is $C_c\approx 15$ nF. For LiPcI the contact resistance varies between 6 Ω and 12 kΩ from room temperature to 20 K, the contact capacitance is 10 nF. In both cases the intrinsic dc resistances R_{dc} were of comparable order of magnitude as R_c. At a given temperature the less

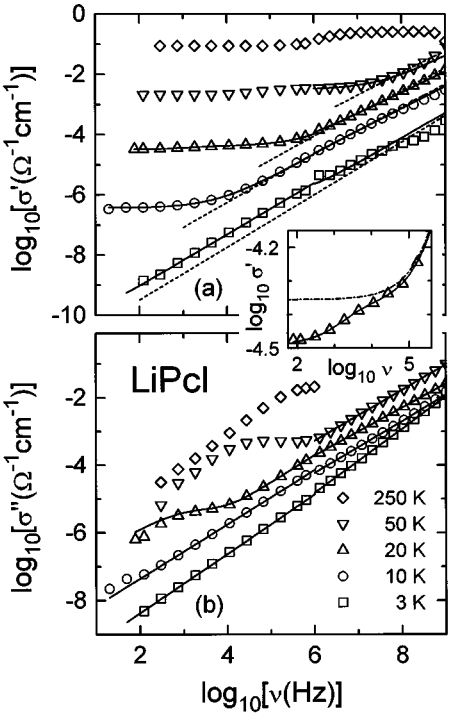

FIG. 4. Frequency dependence of real (a) and imaginary (b) part of the conductivity of LiPcI for various temperatures. The solid lines are the results of fits using the UDR or the equivalent circuit indicated in Fig. 3. The dashed lines in (a) have been calculated according to the OLPT model predictions [Eqs. (1) and (2)] with the parameters obtained from the OLPT fits of the temperature dependent data (Figs. 1 and 2). The inset shows an enlarged view of the behavior at low frequencies at 20 K. The dash–dotted line shows the intrinsic behavior without contacts.

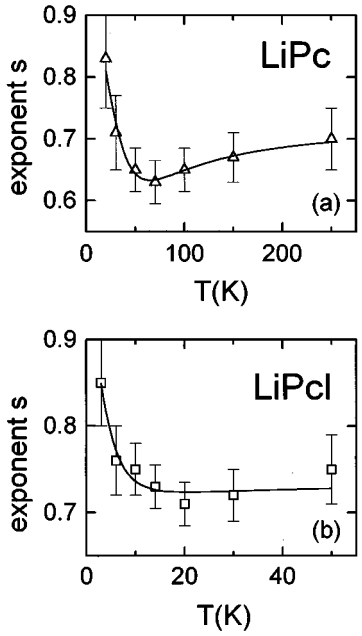

FIG. 5. Temperature dependence of the frequency exponent s for LiPc (a) and LiPcI (b). The solid lines are the results of fits using the OLPT model predictions, Eqs. (1) and (2).

conductive LiPc always exhibited a much higher contact resistance.

An additional feature, seen for LiPcI only, can be understood making a minor addition to the equivalent circuit: At 250 K and for frequencies $\nu>300$ MHz, $\sigma'(\nu)$ decreases again. This is accompanied by negative values of σ'' [not shown in the logarithmic representation of Fig. 4(b)]. This behavior is indicative of inductive behavior and can be modeled by an inductance connected in series to the sample impedance. The influence of the inductance is not seen in the results for LiPc (Fig. 3) which is due to the much higher resistance of this compound.

An increase of the conductivity with frequency has also been reported by Turek *et al.*[13] who performed measurements of the conductivity of tetragonal LiPc at dc and 10 GHz. These authors found a σ' value at 10 GHz which is approximately by one order of magnitude higher than σ_{dc}. This is in agreement with our findings for monoclinic LiPc and is due to the dominance of the dc conductivity up to relatively high frequencies.

Figure 5 shows the temperature dependence of the exponent s as resulting from the fits using the equivalent circuit indicated in Fig. 3. For LiPc, $s(T)$ clearly exhibits a minimum, a behavior which is typical for tunneling of large polarons.[18,19] In the model of "overlapping large polaron tunneling" (OLPT)[19] where the charge carriers are large polarons the lattice distortion around the site of a charge carrier extends over several atomic distances and therefore overlaps with the distortions on neighboring sites. This gives rise to an energy barrier which is a function of the site separation.[19] In the OLPT theory, the temperature dependence of the frequency exponent s is given by

$$s=1-\frac{8\alpha R_W+6\beta W_{\mathrm{HO}}(r_0/R_W)}{[2\alpha R_W+\beta W_{\mathrm{HO}}(r_0/R_W)]^2}. \tag{1}$$

Here W_{HO} is the barrier height for infinite site separation, r_0 is the polaron radius, $1/\alpha$ is the spatial extent of the localized state wave function, and $\beta=1/(k_BT)$. The hopping distance R_W is given by

$$R_W=\frac{1}{4\alpha}\{[\ln(1/\omega\tau_0)-\beta W_{\mathrm{HO}}]+([\ln(1/\omega\tau_0)-\beta W_{\mathrm{HO}}]^2+8\alpha r_0\beta W_{\mathrm{HO}})^{1/2}\}. \tag{2}$$

τ_0 is a characteristic relaxation rate, which should be of the order of a typical phonon frequency. When Eqs. (1) and (2) are used to fit the observed $s(T)$ behavior by least-square fits one obtains the solid lines shown in Fig. 5. A good agreement with the data can be achieved for both materials. The resulting main fit parameters are $W_{\mathrm{HO}}\approx 710$ K, $\omega\tau_0\approx 3.7\times10^{-7}$, and $\alpha r_0\approx 1.7$ for LiPc and $W_{\mathrm{HO}}\approx 100$ K, $\omega\tau_0\approx 2.6\times10^{-7}$, and $\alpha r_0\approx 3.6$ for LiPcI. A problem inherent to this evaluation is traceable to the fact that in the OLPT model the exponent s is slightly frequency dependent [Eq. (1)] while $s(T)$ in Fig. 5 was determined assuming the UDR, i.e., a frequency independent s. Therefore the parameter τ_0 is frequency dependent with a value of $\tau_0\approx 6\times10^{-14}$ s (LiPc) and $\tau_0\approx 4\times10^{-14}$ s (LiPcI) for, e.g., 1 MHz.

The OLPT model also makes distinct predictions concerning the temperature dependence of the ac conductivity σ_{ac}[19]

$$\sigma_{ac}=\frac{\pi^4}{12}\frac{N(E_F)^2(k_BT)^2e^2\omega R_W^4}{2\alpha k_BT+W_{HO}r_0/R_W^2}. \tag{3}$$

Here $N(E_F)$ is the density of states at the Fermi level. The solid lines in Figs. 1 and 2 are the results of fits using Eqs. (2) and (3). Again reasonably good fits have been obtained. The deviations at high temperatures are, in the case of $\sigma'(T)$, due to the increasing dominance of the dc conductivity and/or the contact resistance. For $\epsilon'(T)$ the above mentioned inductance partly suppresses the increase at high temperatures which is most pronounced for LiPcI leading to the saturation near 60 K. Note that the second (high-T) of the two subsequent increases of $\epsilon'(T)$ is completely due to the contact contributions. For both materials a consistent description of the data sets for different frequencies can be obtained with one set of parameters. For LiPc they are: $W_{HO}\approx 900$ K, $\alpha r_0\approx 1.7$, and $\tau_0\approx 1.6\times 10^{-13}$ s. For LiPcI values of $W_{HO}\approx 120$ K, $\alpha r_0\approx 4.7$, and $\tau_0\approx 6.5\times 10^{-16}$ s are found. The parameters W_{HO} and αr_0 have similar values as the ones obtained from the $s(T)$ fits. However, the resulting values of τ_0 are at variance with the findings from the $s(T)$ fits. This discrepancy may well be due to the fact that in the OLPT model a small frequency dependence of s is predicted [Eq. (1)] while the determination of $s(T)$ from our data assumes that s is frequency independent.

Therefore, in order to check for the consistency of frequency and temperature dependence we have calculated the frequency dependence of σ' (without the dc contribution which is not included in the OLPT model) from Eqs. (2) and (3) using the parameters obtained from the fits of the temperature dependent data. The resulting curves are included in Figs. 3(a) and 4(a) as dashed lines and agree reasonably well with the measured data. All these findings lead us to conclude that the OLPT model gives a consistent description of the ac conductivity in LiPc and LiPcI. However, we should mention that the OLPT model does not take into account the one-dimensional character of the charge transport present in LiPc and LiPcI and it is unclear how this property changes the model predictions.

The evaluation of the frequency dependent data using an equivalent circuit, as described above, fixes also the dc conductivity. Its temperature dependence is shown in Fig. 6 for LiPcI in three different representations: $\log \sigma_{dc}$ vs $1/T$, $1/T^{1/2}$, and $1/T^{1/3}$. A straight line is obtained for $\log \sigma_{dc}$ vs $1/T^{1/2}$ only. A behavior

$$\sigma_{dc}=\sigma_0\cdot\exp\left[-\left(\frac{T_0}{T}\right)^{1/\gamma}\right] \tag{4}$$

is indicative of charge transport by tunneling of electrons or holes. In the framework of the variable range hopping (VRH) model,[21] $\gamma=4$ is predicted for isotropic charge transport.[21] A value of $\gamma=2$, as found here, arises for VRH conduction in one dimension, but, however, with the electron wave function still extended over several chains.[21,22] This

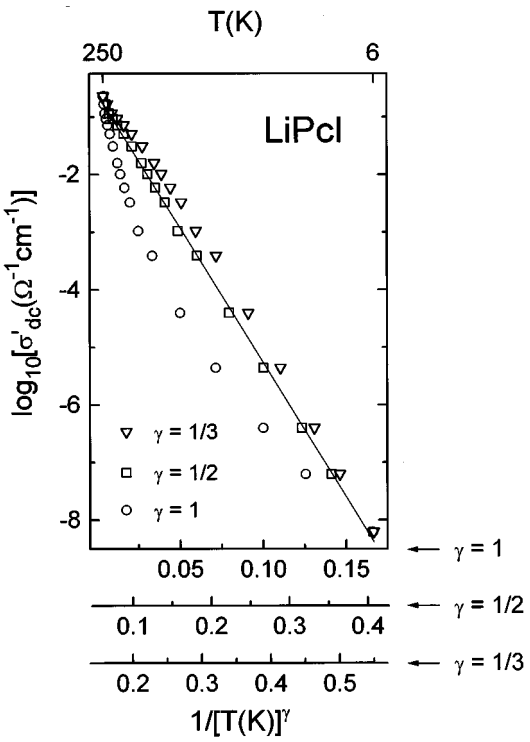

FIG. 6. Temperature dependence of the dc conductivity of LiPcI obtained from the equivalent circuit evaluation described in the text. The data are presented in three different representations, namely vs $1/T$, $1/T^{1/2}$, and $1/T^{1/3}$. The solid line is the result of a fit using Mott's VRH model for one dimension.

quasi-one-dimensional charge transport seems reasonable for LiPcI, because of the stacked structure of the phthalocyanines. However, we want to mention that an alternative explanation of $\gamma=2$ can also be given when in Mott's model for three dimensions the Coulomb interaction between the charge carriers is taken into account.[23]

In Fig. 7 the $1/T^{1/2}$ representation is given for both materials under investigation. In LiPcI this behavior dominates from 4 K up to room temperature. Obviously, LiPc also follows Eq. (4) with $\gamma=2$ but with a different exponential prefactor. The absolute value of the conductivity of LiPc is some orders of magnitude smaller than that of LiPcI. The values of T_0 and σ_0 are 29 000 K and 11 Ω^{-1} cm^{-1} for LiPc and 2600 K and 5 Ω^{-1} cm^{-1} for LiPcI, respectively. T_0 is proportional to $1/r_1N(E_F)$, with r_1 the localization length and $N(E_F)$ the density of states at the Fermi level.[24]

In both materials the dc conductivity at room temperature is significantly higher than that reported previously from dc measurements.[6] As these measurements have been performed using a two-point contact configuration this discrepancy most probably can be ascribed to contributions of the contact resistance. Turek *et al.*[2,13] found a thermally activated behavior of the dc conductivity of tetragonal LiPc crystals between 140 and 300 K. These results, however, were also obtained by using the two-point technique and in addition cover a temperature range which is too small in

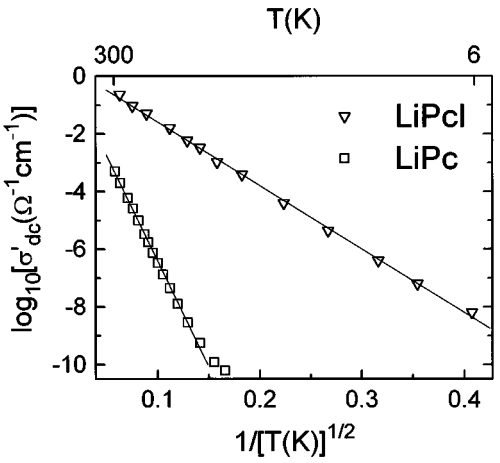

FIG. 7. Temperature dependence of the dc conductivities of LiPc and LiPcI as determined from the equivalent circuit evaluation as described in the text. The data are presented in a way to give a straight line for Mott's VRH in one dimension. The solid lines are linear fits in this representation.

order to get informations on a possible deviation from thermally activated behavior.

IV. CONCLUSIONS

We have investigated the ac electrical properties of monoclinic LiPc and tetragonal LiPcI in a broad frequency range at temperatures down to 1.5 K. The complex conductivity of both materials shows the typical fingerprints of charge transport by hopping between localized sites. Both, the temperature and the frequency dependence can be consistently described using the OLPT model with tunneling of large polarons as dominant charge transport process. The resulting energy barriers separating two localized sites are $W_{HO} \approx 900$ K and $W_{HO} \approx 120$ K for LiPc and LiPcI, respectively. The smaller W_{HO} of LiPcI may well explain the much higher conductivity of the iodinated compound. It is indicative of a better overlap of the π orbitals in this tetragonal compound as compared to the monoclinic LiPc. Therefore we conclude that an increased mobility plays an important role in the enhancement of the conductivity of the iodinated compound and that it is not solely caused by a higher density of charge carriers due to the oxidation of the macrocycles. The high frequency limit of the dielectric constant has been determined as $\epsilon_\infty = 6$ (± 0.5) for LiPc and $\epsilon_\infty = 20$ (± 2) for LiPcI. From a careful evaluation of the frequency dependence using suitable equivalent circuits, we have determined the intrinsic dc conductivity. At room temperature the dc conductivities are $5.3 \times 10^{-4}\ \Omega^{-1}\,\mathrm{cm}^{-1}$ and $0.2\ \Omega^{-1}\,\mathrm{cm}^{-1}$ for LiPc and LiPcI. For both compounds a temperature dependence $\sigma_{dc} \sim \exp[-(T_0/T)^{1/2}]$ has been found which indicates one-dimensional VRH as dominant dc transport mechanism. Even at room temperature, thermal activation of charge carriers across the optical gap is negligible.

ACKNOWLEDGMENT

This work was financially supported by the Max-Planck-Institut für Physik komplexer Systeme (Dresden).

[1] *Phthalocyanines: Properties and Applications*, edited by C. C. Leznoff and A. B. P. Lever (VCH, New York, 1989–1993), Vols. 1–3.
[2] P. Turek, P. Petit, J.-J. André, J. Simon, R. Even, B. Boudjema, G. Guillaud, and M. Maitrot, J. Am. Chem. Soc. **109**, 5119 (1987).
[3] E. Orti, J. L. Brédas, and C. Clarisse, J. Chem. Phys. **92**, 1228 (1990).
[4] K. Yakushi, T. Ida, A. Ugawa, H. Yamakado, H. Ishii, and H. Kuroda, J. Phys. Chem. **95**, 7636 (1991).
[5] P. Turek, J.-J. André, A. Giraudeau, and J. Simon, Chem. Phys. Lett. **134**, 471 (1987).
[6] H. Homborg and C. L. Teske, Z. Anorg. Allg. Chem. **527**, 45 (1985).
[7] H. Sugimoto, M. Mori, H. Masuda, and T. Taga, J. Chem. Soc. Commun., 962 (1986).
[8] M. Hanack and M. Lang, Adv. Mater. **6**, 819 (1994).
[9] L. S. Grigoryan, M. V. Simonyan, and E. G. Sharoyan, Phys. Status Solidi **84**, 597 (1984).
[10] J. Martinsen, S. M. Palmer, J. Tanaka, R. C. Greene, and B. M. Hoffman, Phys. Rev. B **30**, 6269 (1984).
[11] S. Nakamura, H. Amatatsu, T. Ozaki, S. Yamaguchi, and G. Sawa, Jpn. J. Appl. Phys. **26**, 1878 (1987).
[12] T. J. Marks, Science **227**, 881 (1985).
[13] P. Turek, M. Moussavi, P. Petit, and J.-J. André, Synth. Metals **29**, F65 (1989).
[14] R. Böhmer, M. Maglione, P. Lunkenheimer, and A. Loidl, J. Appl. Phys. **65**, 901 (1989).
[15] F. Bensebaa and J.-J. André, J. Phys. Chem. **96**, 5739 (1992).
[16] P. Turek, J.-J. André, and J. Simon, Solid State Commun. **63**, 741 (1987).
[17] P. Turek, M. Moussavi, and J.-J. André, Europhys. Lett. **8**, 275 (1989).
[18] S. R. Elliot, Adv. Phys. **36**, 135 (1987).
[19] A. R. Long, Adv. Phys. **31**, 553 (1982).
[20] A. K. Jonscher, *Dielectric Relaxation in Solids* (Chelsea Dielectrics, London, 1983).
[21] N. F. Mott and E. A. Davis, *Electronic Processes in Non-Crystalline Materials* (Oxford University, Oxford, 1979).
[22] V. K. S. Shante, C. M. Varma, and A. N. Bloch, Phys. Rev. B **8**, 4885 (1973).
[23] B. I. Shklovskii and A. L. Efros, *Electronic Properties of Doped Semiconductors* (Springer-Verlag, Berlin, 1984).
[24] A. N. Bloch, R. B. Weisman, and C. M. Varma, Phys. Rev. Lett. **28**, 753 (1972).